Available online at www.sciencedirect.com
ScienceDirect
Coordination Chemistry Reviews 252 (2008) 2224–2238
COORDINATION CHEMISTRY REVIEWS
www.elsevier.com/locate/ccr

Review

# NMR investigation of non-covalent aggregation of coordination compounds ranging from dimers and ion pairs up to nano-aggregates

Gianfranco Bellachioma, Gianluca Ciancaleoni, Cristiano Zuccaccia, Daniele Zuccaccia, Alceo Macchioni *

*Dipartimento di Chimica, Università di Perugia, Via Elce di Sotto 8, 06123 Perugia, Italy*

Received 12 October 2007; accepted 16 December 2007
Available online 23 December 2007

Dedicated to Professor Giuseppe Cardaci whom we are fortunate to have as our ethical and scientific reference point.

## Contents



**Abstract**

This review summarizes the results recently obtained by our research group investigating the non-covalent aggregation of coordination compounds in solution through NMR spectroscopy. First, systems that can undergo only weak non-covalent interactions, such as dispersive and dipole–dipole ones, are considered; successively, coordination compounds that are capable to establish more energetic non-covalent interactions, such as hydrogen bonding and/or extended π–π stacking interactions, are taken into account. The parallelism between the energy of non-covalent interactions and the level of aggregation is highlighted. The results concerning the latter are mainly obtained through diffusion NMR experiments. In some cases, information about the structure of non-covalent aggregation in solution, obtained through intermolecular NOE studies, is discussed and contrasted with that observed in the solid state (by means of X-ray single crystal investigations, mainly carried out by our group) and/or derived from theoretical calculations.


*Keywords:* Diffusion NMR; Non-covalent interactions; NOE NMR; Organometallic catalysts

## 1. Introduction

The intermolecular (or supramolecular) structure of coordination compounds in solution has been the main object of our studies for the past decade. Its elucidation necessitates the knowledge of two fundamental pieces of information:

* Corresponding author. Fax: +39 0755855598.
*E-mail address:* alceo@unipg.it (A. Macchioni).

0010-8545/$ – see front matter © 2007 Elsevier B.V. All rights reserved.
doi:10.1016/j.ccr.2007.12.016

(1) the relative orientation of the moieties constituting the supramolecule and (2) the average size of the latter. This information can be obtained by means of NMR spectroscopy. Intermolecular nuclear Overhauser effect (NOE) NMR experiments [1], based on the detection of dipolar (through the space) coupling between nuclei, are ideal for obtaining information about the relative orientation of the moiety (1). Diffusion NMR experiments [2] allow the molecular size of the adducts (2) to be estimated. In fact, the average hydrodynamic radius ($r_H$) and volume ($V_H$) of the supramolecule can be evaluated from the translational self-diffusion coefficient ($D_t$) measured, taking advantage of the Stokes–Einstein equation. The latter passage is not devoid of snares but it can be covered if the proper precautions are taken into account [3].

Our attention was first focused on structurally characterizing transition-metal ion pairs in solution, by means of interionic NOE NMR studies, in an attempt to determine the counterion position with respect to the cation [4]. Our interest has been stimulated by the critical role played by ion pairing in several reactions [5], which in some cases are of industrial importance. It was soon demonstrated that interionic NOE NMR techniques were a very powerful tool which not only gives a qualitatively reliable picture of the relative anion–cation orientation but also allows interionic distances to be quantitatively determined [6,7]. Later, we [8] and others [9] realized that diffusion NMR experiments (mainly PGSE, i.e. pulsed field gradient spin–echo) were another equally powerful tool for detecting ion pairing. Although they do not afford any structural information about the ion pairs, they clearly indicate the conditions (solvent, concentration, temperature, etc.) under which ion pairs form. While exploring the effect of changing the solvent and salt concentration, it became clear, always through PGSE NMR studies, that transition-metal ion pairs could aggregate forming ion quadruples and even higher aggregates in solvent with low relative permittivity ($\varepsilon_r$), at relatively high concentration [10,8,11]. Since the considered transition-metal ion pairs did not possess moieties suitable for undergoing hydrogen bonding (HB) or π–π stacking interactions, the aggregation of ion pairs to ion quadrupoles had to be due to the interactions between the permanent dipole moments of two ion pairs. Successive studies were conducted to evaluate the effect of π–π stacking on the aggregation and of introducing proper moieties in the periphery of the coordination compounds that would allow the establishment of other non-covalent intermolecular interactions, particularly HB [12,13]. PGSE NMR studies showed that extensive aggregation occurred in solution [14] for both transition-metal ion pairs and neutral complexes leading, in some cases, to aggregates of nanometric dimensions containing up to hundreds of elemental building blocks [15]. The level of aggregation was conveniently evaluated by defining the aggregation number, $N$, as the observed hydrodynamic volume, $V_H$, over that of the elemental building block ($V_H^0$). The latter coincides with the van der Waals volume ($V_{vdW}$) only for spherical compact molecules without inlets otherwise it is higher than $V_{vdW}$ and usually smaller than the volume derived from X-ray single crystal studies [3]. $V_H^0$ can be evaluated by performing PGSE experiments as a function of the sample concentration by extrapolating the value at infinite dilution, provided that the interaction energy of the elemental units of the supramolecule is not too high [3].

In this paper we review the results of our investigations of the supramolecular structure of coordination compounds in solution using NMR techniques. The focus is limited to systems involving aggregates higher than ion pairs and neutral non-covalent dimers. Transition-metal ion pairs are only considered as the starting points for the aggregative processes since several reviews have recently been published dealing with the application of NOE [6,16,17] and diffusion experiments [16–18] to characterize them. A comparison between the supramolecular structure in solution and that in the solid state is also reported. In some cases, such a comparison is mediated by the results of theoretical calculations that are valuable for highlighting the agreement or the possible differences between them.

Substantially, the subjects are presented following the chronological development of our research. First, the self-aggregation of transition-metal ion pairs that cannot establish intermolecular HB or significant π–π stacking interactions is described. The effect of turning off the dipolar interactions is then faced. In such a case, where only weak dispersive forces are active, it is shown that molecular systems must be large in order for the self-aggregation to occur. Second, coordination compounds with an extended π-electronic conjugation, which sometimes show nanometric aggregates, are considered. Lastly we consider cationic and neutral coordination compounds that have the possibility of undergoing HB and, consequently, exhibit a marked tendency to self-aggregate.

As mentioned above, information on the average hydrodynamic size of the aggregates is obtained through PGSE NMR experiments. Knowing the hydrodynamic size of the constitutive units [19] allows the thermodynamic parameters of the aggregative processes to be determined [3]. In order to furnish a quantitative picture the equilibrium constant and variation of the free energy are given, for most of the examples herein illustrated. Since the forces responsible for the aggregation have been deliberately turned on and off, the quantification can also be useful for evaluating their single contributions.

## 2. Aggregation of ion pairs to ion quadruples and beyond

It is well known that ion pairs, under certain conditions, may undergo self-aggregation forming ion quadruples or higher aggregates through dipole–dipole interactions [20]. Factors that favor aggregation are a large dipole moment of ion pairs, solvents with low relative permittivity and high salt concentrations in solution [21]. Although these conditions were originally discovered for organic ion pairs, they also apply to transition-metal ion pairs. Two other factors must however be taken into account: (i) in cations of coordination complexes, $[ML_n]^{Z+}$, the charge may be highly delocalized onto the ligands (L) since the covalent nature of the M–L bonds involves d-orbitals and (ii) in some cases the cation–anion interaction may have a weak coordinative character. These factors tend to reduce the dipole moment of the ion pairs and, consequently, decrease their tendency to self-aggregate.

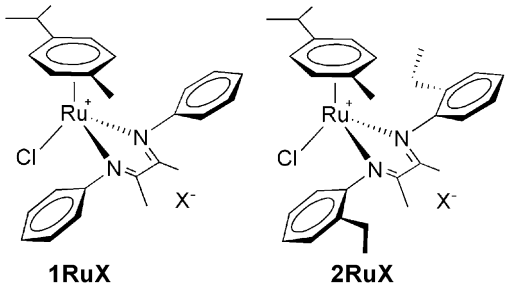


X = $BF_4$, $PF_6$, $CF_3SO_3$, $BPh_4$, $B(3,5\text{-}(CF_3)_2C_6H_3)_4$ (BARF)

Scheme 1.

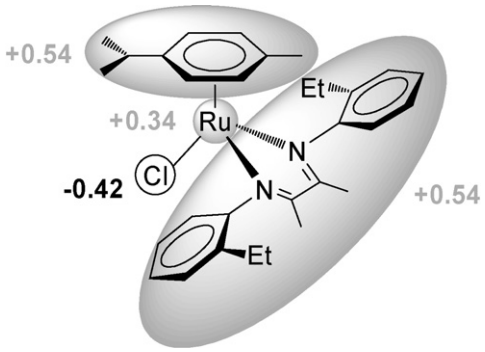


Fig. 2. Schematic representation of the charge distribution in **2Ru**$^+$.

In the following, some recent examples of self-aggregation in some ruthenium and zirconium transition-metal salts are presented. While other types of weak forces may play some minor roles, self-association of the resulting ion pairs is mainly driven by dipole–dipole and dipole–multipole interactions.

### 2.1. Aggregation of arene Ru(II) ion pairs

Recent PGSE NMR measurements showed that aggregates larger than ion pairs are formed by half-sandwich ruthenium-diimine salts (Scheme 1) in solvent with a relative permittivity lower than that of chloroform ($\varepsilon_r^{20\,^\circ C} = 4.81$) [11,22].

This is illustrated in Fig. 1, where cationic aggregation numbers ($N^+$) [23] are reported as a function of the concentration ($C$) for complexes **1Ru**$BPh_4$ in methylene chloride (■) and chloroform (▲) and for **1Ru**$PF_6$ in benzene (○ ). As expected, an increase in the salt concentration favors both ion pairing (**1Ru**$BPh_4$ in methylene chloride, Fig. 1) and ion quadrupoling (**1Ru**$PF_6$ in benzene, Fig. 1).

Although the low solubility of some salts prevented a complete study, some interesting trends were observed regarding their tendency to form ion quadruples as a function of the size of the ions. Considering the same cation, larger counterions favor the formation of ion quadruples. This is evident when different salts at similar concentrations are compared: at 5 mM in benzene, $N^+ = N^- = 1.2$ for **1Ru**$PF_6$ and $N^+ = N^- = 2.1$ for **1Ru**BARF (BARF = $B(3,5\text{–}(CF_3)_2C_6H_3)_4$) while, at 32 mM in chloroform, $N^+ = 1.5$ and $N^- = 1.3$ for **2Ru**$BF_4$, $N^+ = 1.6$ and $N^- = 1.5$ for **2Ru**$CF_3SO_3$ and $N^+ = N^- = 1.9$ for **2Ru**$BPh_4$ [23]. It also seems that larger cations favor ion-quadrupoling: for example, **2Ru**$BF_4$ ($N^+ = N^- = 1.9$) shows a slightly larger aggregation than **1Ru**$PF_6$ ($N^+ = 1.7$, $N^- = 1.5$), in benzene at ca. 36 mM. A rationale for the observed trends can be drawn by taking into account that the dipole moment of the ion pair increases on passing from small to large counterions. As stated above, when organometallic cations are considered, the charge distribution may be highly unsymmetrical. The latter was estimated for the cation **2Ru**$^+$ by means of natural population analysis (NPA) calculations (Fig. 2) [24].

Small counterions, like $BF_4^-$ and $PF_6^-$, can dock closely with the cation from the side of the *N*,*N* ligand, just above the bridging diimine carbon atoms (Fig. 3, orientation A). From this location the anions can interact with the partial positive charge present on both the diimine ligand and the cymene moiety. Such a preferential position was observed experimentally both in solution by $^{19}F,^1H$-HOESY NMR spectroscopy as well as in the solid state by X-ray investigations. Our *n*-layered integrated molecular orbital and molecular mechanics (ONIOM) [25] calculations indicated that the energy of the cation–anion orientation A is 8.8 kcal mol$^{-1}$ less than that of orientation B, where the anion is

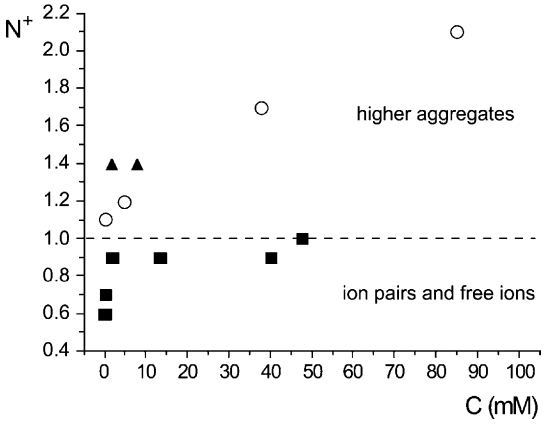


Fig. 1. Cationic aggregation numbers ($N^+$) as a function of salt concentration ($C$). **1Ru**$BPh_4$ (methylene chloride-$d_2$, ■), **1Ru**$BPh_4$ (chloroform-$d$, ▲), **1Ru**$PF_6$ (benzene-$d_6$, ○ ).

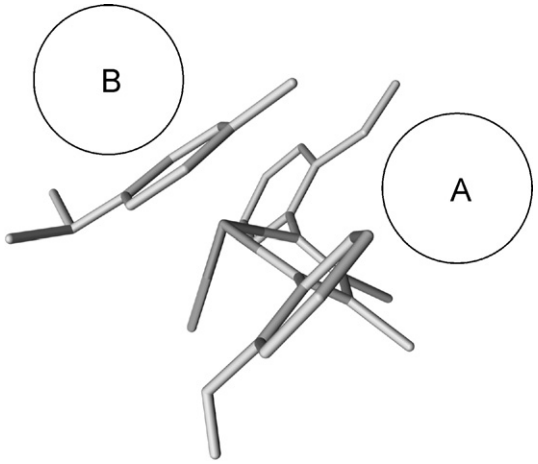


Fig. 3. Schematic representation of the two cation–anion orientations in **2RuX**.

totally shifted to the side of the cymene moiety. The calculated dipole moment for the most stable ion pair is 15D [22].

In sharp contrast, for large counterions like $BPh_4^-$ and $BARF^-$, that cannot approach closely the cation, the two orientations have similar energies, with a $\Delta E$ of about 1.7 kcal mol$^{-1}$, as estimated from ONIOM calculations. In addition, since the anion is much more distant from the cation, the dipole moments for both orientations are much higher (30D). The 15D difference between the dipole moment values of the ion pairs with small and large counterions could explain their different aggregation tendencies. In agreement, for complexes bearing $BF_4^-$ or $PF_6^-$, the equilibrium constant for ion quadruples formation ($K_{IQ}$) is 40–100 M$^{-1}$ ($-\Delta G^0_{IQ} = 2.0$–$2.8$ kcal mol$^{-1}$) in chloroform, while it increases to 200–700 M$^{-1}$ ($-\Delta G^0_{IQ} = 3.1$–$3.8$ kcal mol$^{-1}$) when $BPh_4^-$ salts are considered, in the same solvent [3]. DFT calculations, carried out for a simplified ion pair similar to **1Ru**$BF_4$ having benzene instead of cymene (**3Ru**$BF_4$), indicate that the formation of an ion quadruple from two ion pairs is an exothermic process with a $\Delta E \approx 6$–$12$ kcal mol$^{-1}$ in gas phase and 2.4–4.8 kcal mol$^{-1}$ in dichloromethane.

The structure of ion quadruples was investigated by an integrated approach based on NOE NMR spectroscopy, X-ray diffraction studies and theoretical calculations and it was found that the structure is strictly related to the nature of the anion. The conditions required to have a substantial amount of ion quadruples in solution can be determined from PGSE data, while the interionic structure of the aggregates can be investigated by $^1$H-NOESY and $^{19}$F,$^1$H-HOESY spectroscopy. As mentioned before, $^{19}$F,$^1$H-HOESY experiments indicate that the anion is located above the diimine carbons (orientation A in Fig. 3) when ion pairs with small counterions are present in solution (**2Ru**$BF_4$, $CD_2Cl_2$, 34.1 mM). Some changes can be observed in the relative interionic NOE intensities in the $^{19}$F,$^1$H-HOESY spectra recorded under conditions where ion quadruples are the predominant species (**2Ru**$BF_4$, $C_6D_6$, 34.1 mM) (Fig. 4); the changes are consistent with an average shift of the counterion toward the cymene moiety. The interionic structure of ion pairs with larger counterions shows less selectivity in the NOE contacts (**2Ru**$BPh_4$, $CD_2Cl_2$, 43 mM). Again there is a good agreement with the results derived from calculations that predicted similar stabilities in the A and B orientations (Fig. 3) for **2Ru**$BPh_4$.

No changes in the relative NOE intensities were observed when ion quadruples were mainly present in solution for ion pairs with large counterions. Given that an alternation in the cations and anions is also found in the solid-state structures of **1Ru**$BPh_4$ and **2Ru**$BPh_4$ [22], a head-to-tail arrangement of the type [Ru$^+$X$^-$Ru$^+$X$^-$] is more probable in the large anion-bearing ion quadruples. In contrast, both head-to-head [X$^-$Ru$^+$Ru$^+$X$^-$] and tail-to-tail [Ru$^+$X$^-$X$^-$Ru$^+$] ion quadruples, differing with respect to both disposition and orientation of the ionic moieties, are found in the solid state for salts containing small fluorinated anions (Fig. 5). DFT calculations, carried out for **3Ru**$BF_4$ in the gas phase, indicate that the [Ru$^+$X$^-$X$^-$Ru$^+$] arrangement is favored (Fig. 5, left). Nevertheless, inclusion

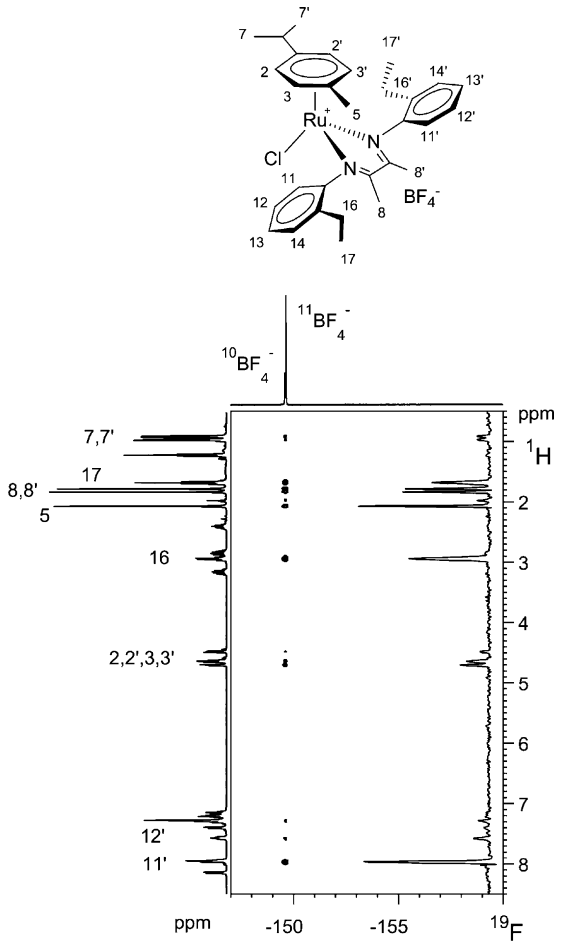


Fig. 4. $^{19}$F,$^1$H-HOESY spectrum for **2Ru**$BF_4$ ($C_6D_6$, 296 K, 34.1 mM).

of the solvent ($CH_2Cl_2$) as a continuum, reduces the energy difference between the structurally different quadruples to the point that the actual geometry may critically depend on the steric requirements of both cation and anion.

### 2.2. Aggregation of zirconocene ion pairs

Metallocenes have a relevant position in the field of homogeneous olefin polymerization catalysis [26]. It is now widely accepted that ion pairs of general structure [Cp$^R_2$MR]$^+$X$^-$ are the catalytically active species. Considering that olefin polymerization reactions are usually conducted in solvents with a very low relative permittivity, like benzene ($\varepsilon_r^{20°C} = 2.28$), toluene ($\varepsilon_r^{23°C} = 2.38$) or isoparaffins ($\varepsilon_r < 2.00$), the earlier assumed mechanism in which the ion pair dissociates in solution to generate the highly active 14-electron cation [Cp$^R_2$MR]$^+$ seems unlikely. On the contrary, association of ion pairs to ion quadruples or higher aggregates may occur. PGSE NMR experimental evidence for ion pair aggregation in zirconocene complexes was first reported by Brintzinger and co-workers [10]. A few years later, we carried out an extensive PGSE investigation [27] in collaboration with Marks and co-workers, in which we studied a number of zirconocene ion pairs in benzene, varying the metallocene skeleton, nature and size of the anion and salt con-

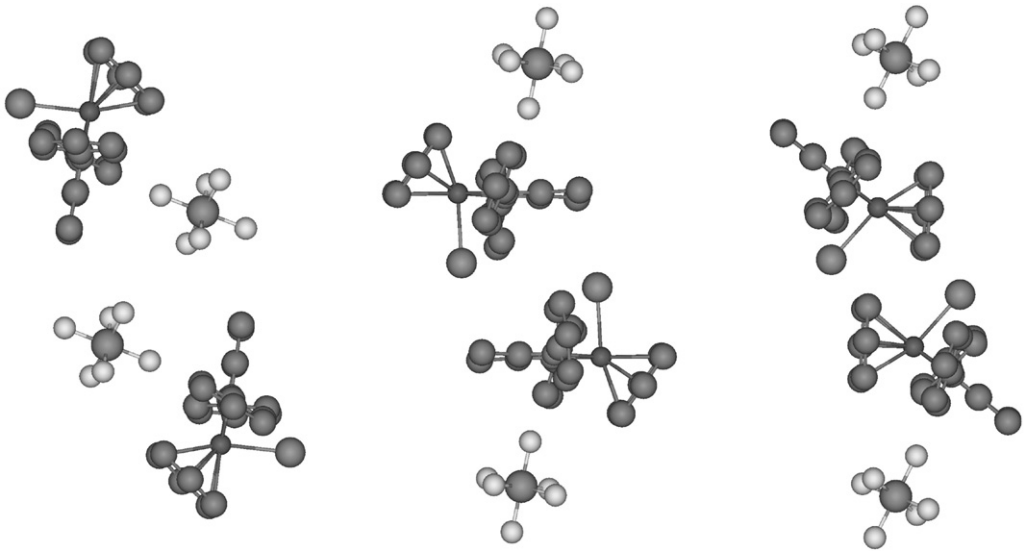

Fig. 5. Ion quadruples observed in the solid state of **3Ru**$PF_6$.

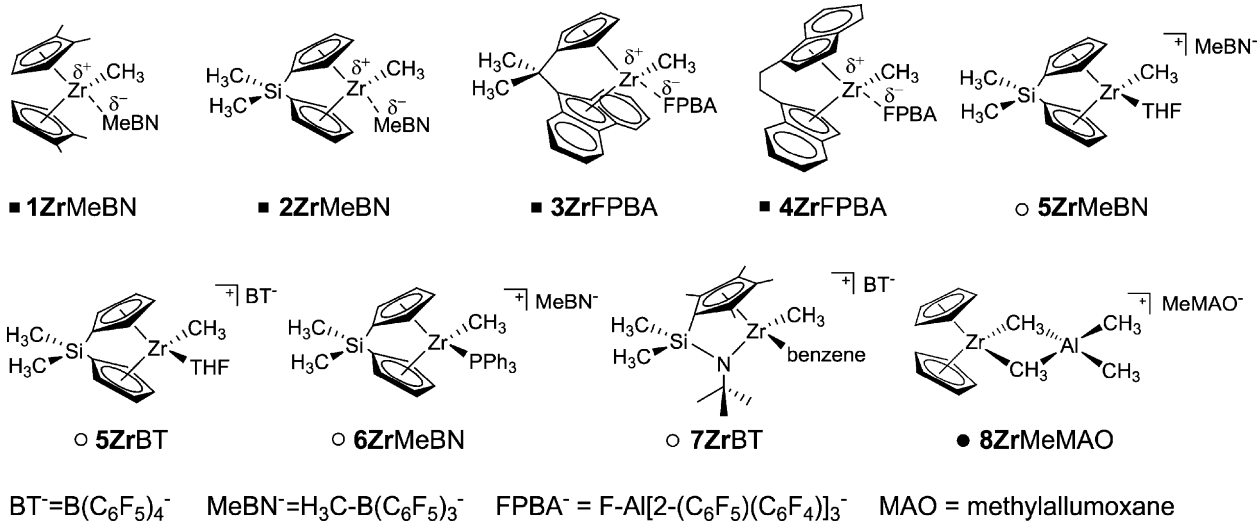


Scheme 2.

centration. Both inner sphere (ISIP) [5] and outer sphere (OSIP) [5] contact ion pairs were studied (Scheme 2).

The trends of the aggregation number as a function of salt concentration, for ion pairs shown in Scheme 2, are illustrated in Fig. 6 [28]. There is no evidence of aggregation in any of the ISIPs up to a concentration of ca 10 mM, irrespective on the size of the ions. This can be reasonably attributed to the fact that the dipole moment of the ISIPs is small since, by definition, the anion occupies one of the coordination sites and, consequently, it closely approaches the cation. As far as the anion orientation is concerned, it is known that the methyl group bonded to the boron atom in $MeBN^-$ ($MeBN^- = MeB(C_6F_5)_3^-$) and the fluorine atom bonded to the aluminium atom in $FPBA^-$ ($FPBA^- = FAl[2(C_6F_5)(C_6F_4)_3]^-$) are directed toward the otherwise free coordination site of the corresponding zirconocenium cations [29]. The results of $^1$H-NOESY and $^{19}$F,$^1$H-HOESY NMR investigations showed that this anion orientation is maintained in solution for both ion pair

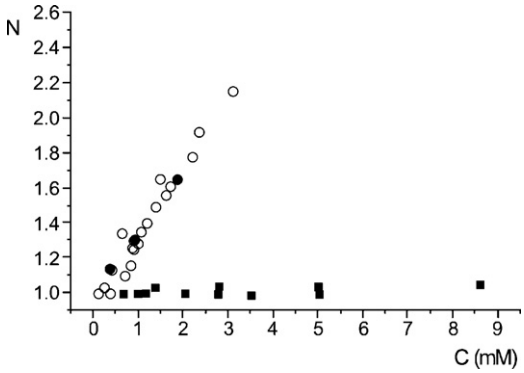


Fig. 6. Aggregation number ($N$) as a function of concentration ($C$) for zirconocene ISIPs (■) and OSIPs (○) shown in Scheme 2 and $[Cp_2Zr(\mu\text{-}Me)_2AlMe_2]^+MeMAO^-$ (●) in benzene-$d_6$.

**2Zr**MeBN and **4Zr**FPBA [27]. Recent calculations, carried out on systems containing the $MeB(C_6F_5)_3^-$ anion, showed that the cation–anion interaction in these ion pairs is primarily electrostatic in nature [30], but some residual directional coordinative interaction cannot be excluded.

In sharp contrast, the hydrodynamic volume of outer-sphere ion pairs **5Zr**MeBN, **5Zr**BT ($BT^- = B(C_6F_5)_4^-$), **6Zr**MeBN and **7Zr**BT increases markedly with increasing concentration. Although the highest $N$ value of each OSIP is different and depends on the solubility, the $N$ *versus* $C$ trends are similar. In addition, the slope of $N$ *versus* concentration is rather steep for all the ion pairs and does not reach a *plateau* at values around 2. This suggests that aggregation may proceed beyond ion quadrupoling. Fitting the experimental data with the equation derived from the equal constant model (EK) [31] gives a rough $K_{IQ}$ estimate of ca. 1000 $M^{-1}$, which corresponds to a $\Delta G^0$ of about −4.0 kcal $mol^{-1}$. In OSIPs, the anion is located in the second coordination sphere and, consequently, an increase in the ion pair dipole moment is expected. In agreement, both experimental [27] and theoretical [32] data indicate a drastic interionic structural rearrangement on passing from **2Zr**MeBN to **5Zr**MeBN. As stated above, in **2Zr**MeBN the methyl group bonded to boron steadily points toward the free coordination site at the zirconium center, resulting in a Zr–B distance around 4.2 Å and a Zr–Me–B angle around 175°; in **5Zr**MeBN the average Zr–B distance is ca. 7.2 Å, and, more importantly, the B–Me bond points away from the metal (Zr–Me–B angle ≈ 0°). As a consequence, the three $C_6F_5$ groups of the $MeBN^-$ anion face the metallocene, resulting in a cation–anion orientation that is very similar to that of **5Zr**BT which contains the $C_6F_5$-tetra-substituted anion. This explains why they have a similar tendency to self-aggregate.

A few other studies concerning self-aggregation of metallocenium ion pairs have been reported in the literature. Babushkin and Brintzinger used PGSE NMR methods to estimate the dimensions of the $MeMAO^-$ anion by measuring the diffusion coefficient of the ion pair $[Cp_2Zr(\mu\text{-}Me)_2AlMe_2]^+$ $MeMAO^-$ (**8Zr**MeMAO), which is formed upon the activation of $Cp_2ZrMe_2$ with MAO [33]. The effect of the total concentration was investigated, but the results in terms of ion pair self-aggregation are strongly puzzled by the use of different Zr/Al ratios and the intrinsic nonuniformity of the MeMAO anion. Some data can be extracted at a constant Al/Zr ratio (Al/Zr = 60) [34] and compared with the results presented above. For **8Zr**MeMAO, aggregation numbers $N = 1.6$ (1.88 mM), 1.3 (0.92 mM) and 1.1 (0.36 mM) are obtained, which give $K_{IQ} = 615\ M^{-1}$ and $\Delta G^0 = -3.8$ kcal $mol^{-1}$. In spite of the marked increase of the anion size on passing from perfluoroarylborate anions to $MeMAO^-$, it appears that the tendency of **8Zr**MeMAO to self-aggregate is similar to that of other OSIPs. A possible explanation can be found by considering the anion charge distribution and anion–cation orientations in **8Zr**MeMAO. In the cage structure of $MeMAO^-$, the negative charge may remain substantially localized, and it may reside on the peripheral –O–$AlMe_3$ moiety which is formed after methyl abstraction by an –O–$AlMe_2$. [35] Then, it is reasonable that the $MeMAO^-$ anion orients the –O–$AlMe_3$ moiety toward zirconium in the **8Zr**MeMAO ion pair (Fig. 7). Consequently, the dipole moment and the self-aggregation tendency of the ion pair will be quite similar to that of other zirconocene OSIPs.

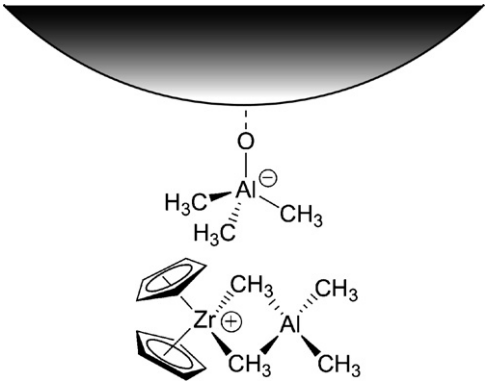


Fig. 7. Schematic representation of the possible preferred anion–cation orientations in the ion pair **8Zr**MeMAO.

In collaboration with Bochmann and co-workers, we more recently reported some PGSE studies on strictly related *ansa*-metallocene ion pairs bearing the bulky $-CH_2SiMe_3$ alkyl group (Scheme 3) [36,37].

When the cation is paired with the sticky $MeBN^-$ anion, the bulky alkyl ligand points away from the metal and the corresponding ISIPs, **9Zr**MeBN and **10Zr**MeBN, are obtained. In agreement with previous findings, these ion pairs show a negligible tendency to self-aggregate. Outer-sphere ion pairs **11Zr**BT and **12Zr**BT are obtained when the least coordinating $BT^-$ anion is used. In these species, the agostic γ-$CH_3$ interaction with one methyl of the $SiMe_3$ group stabilizes the unsaturated metal center and prevents the anion coordination. In toluene, complex **11Zr**BT exhibits $N = 1.4$ [38] at 1.6 mM (saturated solution), in good agreement with other metallocenium OSIPs (Fig. 6). Increasing the concentration (up to 10 mM) and the solvent polarity (toluene/1,2-$F_2C_6H_4$, 90/10 in volume) results in an aggregation number of 2.2 [38]. In comparison with the trends reported in Fig. 6, the increased relative permittivity of the medium diminishes the

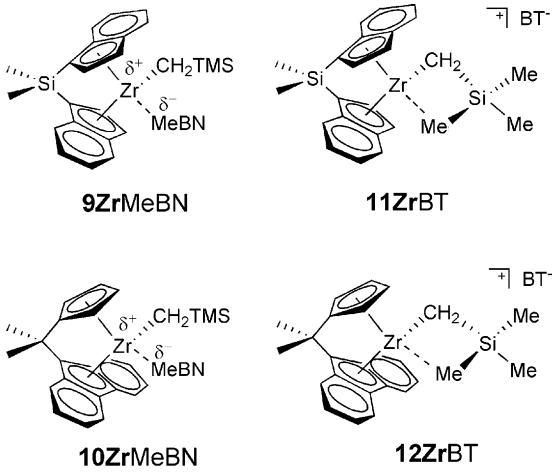


$MeBN^- = H_3C\text{-}B(C_6F_5)_3^-$ ; $BT^- = B(C_6F_5)_4^-$

Scheme 3.

self-aggregation tendency of **11Zr**BT. Consistently, the aggregation number of both **11Zr**BT and **12Zr**BT is further reduced to 1.8–1.9 at 7 mM when the measurements are performed in toluene/1,2-$F_2C_6H_4$ (80/20 in volume). Interestingly, the addition of an excess of $[CPh_3]^+[B(C_6F_5)]_4^-$ to solutions of both **11Zr**BT and **12Zr**BT leads to the formation of mixed ion aggregates of the type $[\{Cp_2{}^RZrR^+\}_{n-}\{CPh_3^+\}_m\{B(C_6F_5)_4^-\}_{(n+m)}]$ [37]. In fact, at constant metallocene concentration (7 mM), the $V_H{}^+$ of both **11Zr**BT and **12Zr**BT increases on increasing the concentration of $[CPh_3]^+[B(C_6F_5)]_4^-$, passing from 1700–1800 to 2100–2200 Å$^3$ after adding a fourfold excess of tritylborate.

It has been proposed that the formation of ion quadruples and/or higher aggregates may explain the increment of the site epimerization rate observed when the metallocenium concentration is increased [39,36] as well as the substantial enhancement of the catalytic activity when an excess of ionic activators is used [40,37]. Moreover, it has been suggested that the ion quadruple, and not the ion pair, may be the real active catalyst [41]. Taking an average $K_{IQ} = 1000\ M^{-1}$ (see above), the concentration of ion quadruples is $10^3$ to $10^4$ times lower than that of the single ion pair under typical catalytic conditions (catalyst concentration = $10^{-6}$ to $10^{-7}$ M); in other words, ion quadruples would be relevant in catalysis only if they have a reactivity that is markedly higher than that of the ion pairs.

Another subtle aspect related to the aggregation of organometallic ion pairs needs to be outlined. As stated above, the counterion plays a critical role in several processes catalyzed by transition-metal salts [5], also finely tuning the Lewis acidity of the metal center and, consequently, its ability to bind a substrate. Therefore, several efforts have been made in "anion engineering" [29,42] to reduce anion–cation interactions. A reduced anion nucleophilicity is usually achieved by delocalizing the negative charge over as large a volume as possible. It should be considered that this can lead to a higher charge separation in ion pairs with a consequent increased molecular dipole moment and greater tendency to self-aggregation [22].

## 3. "Switching off" the dipole–dipole interaction

An aggregation tendency similar to that of arene Ru(II) and zirconocene ion pairs was previously observed for the octahedral complex *trans*-[Ru(COMe){$(pz_2)CH_2$}(CO)$(PMe_3)_2$]$BPh_4$ (pz = pyrazol-1-yl-ring) in $CDCl_3$ [8]. Also in this case, the association of two ion pairs to form ion quadruples is reasonably driven by the dipole–dipole interaction since no functionality suitable to HB or substantial π–π stacking appears to be present in the cationic moiety. Consistently, the isosteric and isoelectronic neutral analog of the cationic fragment, *trans*-[Ru(COMe){$(pz_2)BH_2$}(CO)$(PMe_3)_2$], does not show any tendency to aggregate even at relatively high concentration values [8,12]. This means that when the dipole–dipole interaction is also "switched off" the remaining dispersive forces are not strong enough to cause self-aggregation. If this is true for small molecules, it does not seem to be for large molecular systems that are capable of establishing a network of weak dispersive forces that act cooperatively.

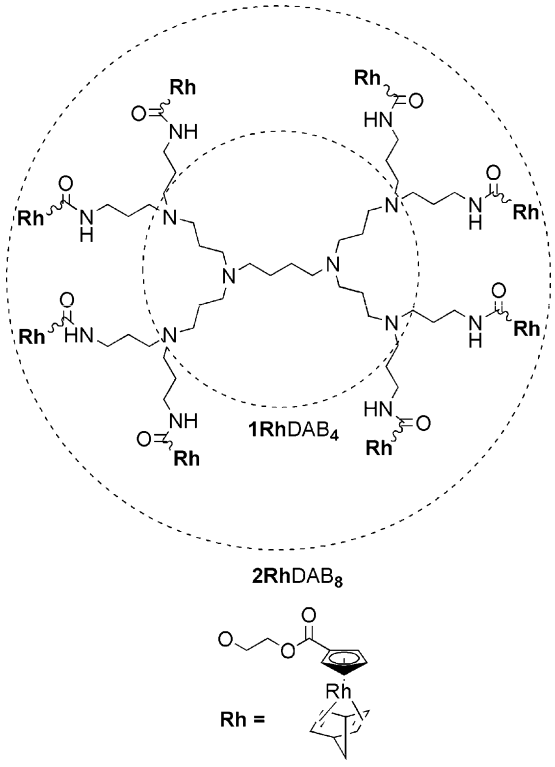


Scheme 4. Schematic representation of DAB-*dendr*-[NH(O)$COCH_2CH_2OC$(O)$C_5H_4$Rh(NBD)]$_n$ ($n$ = 4, **1Rh**$DAB_4$; 8, **2Rh**$DAB_8$).

In fact, a systematic PGSE NMR study [43], conducted in collaboration with Busetto and co-workers on both the poly(propylenimine) dendrimers (DAB-*dendr*-$(NH_2)_n$, $n$ = 4, $DAB_4$; 8, $DAB_8$; 16, $DAB_{16}$; 32, $DAB_{32}$; 64, $DAB_{64}$; DAB = diaminobutane) and their organometallic derivatives DAB-*dendr*-[NH(O)$COCH_2CH_2OC$(O)$C_5H_4$Rh(NBD)]$_n$ ($n$ = 4, **1Rh**$DAB_4$; 8, **2Rh**$DAB_8$; 16, **3Rh**$DAB_{16}$; 32, **4Rh**$DAB_{32}$; 64, **5Rh**$DAB_{64}$; Scheme 4; NBD = norbornadiene) [44], shows that the highest generations self-aggregate to form dimeric megamers. Aggregation numbers of DAB-organo-rhodium dendrimers in $CD_2Cl_2$ as a function of the

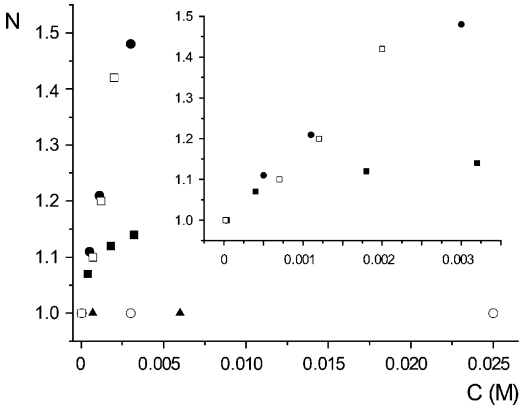


Fig. 8. Aggregation number ($N$) as a function of the concentration ($C$) in $CD_2Cl_2$. **1Rh**$DAB_4$ (○), **2Rh**$DAB_8$ (▲), **3Rh**$DAB_{16}$ (■), **4Rh**$DAB_{32}$ (●), **5Rh**$DAB_{64}$ (□). On the right an expansion relative to the $N$ dependence on $C$ for the highest generations is reported.

concentration are shown in Fig. 8. The dimensions of the first three generations are independent of the concentration with $N$ oscillating between 1.0 and 1.1. In contrast, the $N$ value increases with the concentration for the two highest generations and approaches 1.5 already at 3 mM.

The aggregation process appears to be an intrinsic feature of the dendrimeric skeleton, with the organometallic fragment playing a minor role. In fact, $N$ is ca. 1 for $DAB_4$, $DAB_8$ and $DAB_{16}$ up to 15 mM, while it increases to 1.5 and 1.7 for $DAB_{32}$ and $DAB_{64}$ in the same concentration range [43]. In addition, the organometallic mononuclear precursor $HOCH_2CH_2OC(O)C_5H_4Rh(NBD)$ (**6Rh**) does not show any tendency to aggregate up to 100 mM in $CD_2Cl_2$. The dimerization equilibrium constant ($K_D$) in $CD_2Cl_2$ can be estimated using the monomer/dimer model [3]. The $K_D$ values for **4Rh**$DAB_{32}$ and **5Rh**$DAB_{64}$ are 500 $M^{-1}$ ($\Delta G^0 = -3.7$ kcal $mol^{-1}$) and 600 $M^{-1}$ ($\Delta G^0 = -3.7$ kcal $mol^{-1}$), respectively.

## 4. Aggregation driven by extended π–π stacking interaction

The attractive interaction derived from the π–π stacking of aromatic moieties [45] plays a relevant role in supramolecular [46–48] and biomolecular [49,50] sciences. Focusing on coordination complexes, luminescent polypyridyl metal complexes are one of the most important classes of compounds whose structure and behavior are strongly affected by π–π stacking interaction. These complexes have attracted considerable attention due to their photophysical and redox properties [51,52], as well as their capability to interact with DNA [53]. Their self-aggregation has been extensively investigated by optical and NMR spectroscopies. For instance, Kol and co-workers studied the stereospecific dimerization of some $[Ru(N,N)_2(eil)][PF_6]_2$ complexes (eil = eilatin) in acetonitrile, and found that the equilibrium constant for the dimerization ranged from 10 to 1000 $M^{-1}$ depending on the extension of the aromaticity [54].

The self-aggregation tendency is much more pronounced on passing from octahedral to square planar complexes. This is probably because the latter can undergo metal-metal interactions [55] and a better π–π stacking of the polypyridyl ligands due to a reduced steric hindrance in the apical positions. This, on the one hand, leads to a much higher $K_D$ as found by Romeo and co-workers investigating $[Pt(terpy)(CH_3)]^+Cl^-$ (**1Pt**Cl, terpy = 2,2′:6′,2″-terpyridine) in aqueous solution ($K_D = 26{,}000\ M^{-1}$ at 298 K, $\Delta G^0 \approx -6$ kcal $mol^{-1}$) [56]. On the other hand, it can lead to the formation of more extended aggregates [57,58].

We have verified this by investigating the self-aggregation tendency of the dinuclear palladium complex $[(Phen)_2Pd_2(\mu\text{-}H)(\mu\text{-}CO)]^+BARF^-$ (**1Pd**BARF, Scheme 5) in nitrobenzene by means of PGSE NMR diffusion experiments and UV–vis spectroscopy [14]. **1Pd**BARF has a remarkable tendency to form aggregates in solution. PGSE measurements indicated that the hydrodynamic volume of the cation increases ca. fourfold on varying the concentration from 0.43 to 55 mM, while that of the anion remained rather constant, i.e. the cationic units of **1Pd**$^+$ were involved mainly in the aggregation process.

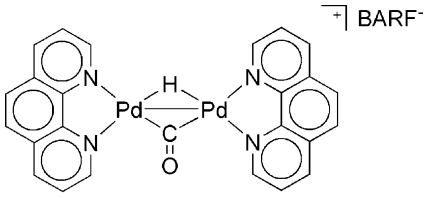


**1PdBARF**

Scheme 5.

Both techniques used indicate that two different aggregation processes are active that have completely different energies. The most energetic pathway was responsible for the formation of the dimeric species that was always detectable even at the lowest concentrations. Elaborating the diffusion data according to the modified isodesmic model of indefinite association, in which $K_D$ differs from the association constant ($K$) of higher aggregation [31], leads to $K_D = 180{,}000\ M^{-1}$ and $K = 15{,}000\ M^{-1}$.

## 5. Aggregation driven by hydrogen bonding

HB is probably the most important non-covalent weak interaction [59]. A simple definition of the hydrogen bond that includes classical and non-classical views is "*an X–H···A interaction is called a hydrogen bond, if (i) it constitutes a local bond, and (ii) X-H acts as proton donor to A*." [59]. While the strength of the interaction is variable and depends on the molecular system and the environment, it usually ranges between a few and 40 kcal $mol^{-1}$ [60]. An important feature of HB is the so-called σ-bond cooperativity that drives the clustering of polar groups [60]. It stems from the fact that when an $X^{\delta-}$-$H^{\delta+}$ group forms a hydrogen bond $X^{\delta-}$–$H^{\delta+}\cdots A^{\delta-}$, it becomes more polar. Consequently, in a chain with two hydrogen bonds, such as Y–H···X–H···A, *both* become stronger.

HB strongly contributes to determine the structure [61] and reactivity of coordination compounds. It has been used to develop molecular receptors for anion [62], cation [63] and ion pairs [64], and improve the performances of organometallic [65] and bio-organometallic [66] catalysts. It is reasonable that coordination compounds, capable of establishing intermolecular HB, self-aggregate in solution. In the following sections, recent examples of hydrogen bond-driven self-aggregation of ionic and neutral ruthenium compounds are presented.

### 5.1. Aggregation of cationic arene Ru(II) complexes

As described in Section 2, dipole–dipole interactions are mainly responsible for the self-aggregation of transition-metal ion pairs into ion quadruples, or larger aggregates, in solvents with low relative permittivity. In solvents with moderate to high relative permittivity, free ions and ion pairs are the predominant species unless the cation and anion have suitable moieties to undergo intermolecular interactions. In order to explore the effect of intermolecular HBs on the self-aggregation tendency of ionic species we designed and synthesized two classes of

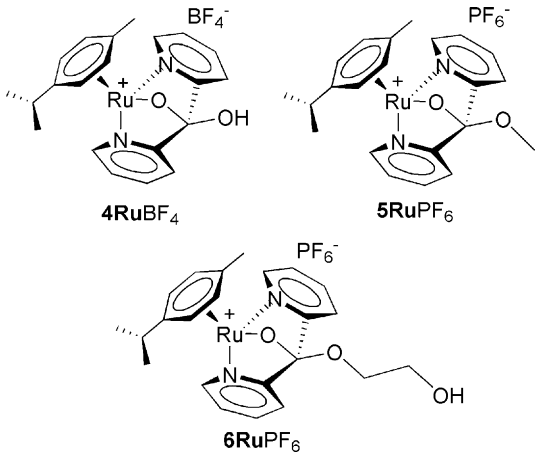


Scheme 6.

ruthenium(II) arene salts with HB donor and HB acceptor functionalities in the first (Cl, O, $NH_2$) and second (OH) coordination sphere of the metal.

### 5.1.1. Arene Ru(II) complexes with the dpk ligand

The interionic structure of complexes [Ru(arene)($\kappa^3$-dpk-OR]X (dpk = 2,2′-dipyridylketone, **4Ru**$BF_4$, **5Ru**$PF_6$ and **6Ru**$PF_6$, Scheme 6) was investigated through an integrated approach based on X-ray, PGSE NMR diffusion and NOE NMR studies [67].

PGSE and NOE NMR results indicated that the aggregation tendency of **4-6Ru**X complexes strongly depends on the nature of the OR-tail. The highest aggregation tendency is found for complex **4Ru**$BF_4$ that shows aggregation numbers consistent with the main presence of ion triples $Ru_2X^+$ ($N^+ = 1.9$ and $N^- = 1.1$) in $CD_2Cl_2$, even at low concentration (0.5 mM). The aggregation level of **4Ru**$BF_4$ increases as the concentration increases; in the saturated solution (1.7 mM) the formation of ion quadruples becomes significant ($N^+ = 2.2$ and $N^- = 1.7$). X-ray investigations of **4Ru**$BF_4$ indicated that a [1 × 1] network of HBs is present that involves the OH moieties of the two cationic fragments belonging to the two independent ion pairs of the asymmetric unit (Fig. 9A). Moreover, their pyridyl rings undergo a π–π stacking interaction. It is reasonable to believe that the dication observed in the solid state is the central moiety of the $Ru_2X^+$ ion triples that was evidenced by PGSE NMR experiments. NOE NMR spectroscopy supports the formation of this rare example of $Ru_2X^+$ ion triples driven by intercationic HBs. Specifically, the intensities of the interionic contacts follow the rather peculiar order H8 ≈ H10 > H9 ≈ H11 in the $^{19}F,^1H$-HOESY NMR spectrum indicating that the counterion is located close to the two pyridyl rings involved in the intercationic π–π stacking interaction (Fig. 9B).

**5Ru**$PF_6$ has about the same tendency to aggregate as **6Ru**$PF_6$ in $CD_2Cl_2$ but much less than **4Ru**$BF_4$ and analogous to that of **1Ru**X and **2Ru**X (X = $BF_4$ or $PF_6$). This means that ion pairing is the main aggregative process in methylene chloride [22]. While it is reasonable that **5Ru**$PF_6$, not having the possibility for HB, aggregates less than **4Ru**$BF_4$, it could appear surprising that **6Ru**$PF_6$ behaves similarly. A rationale can be found in

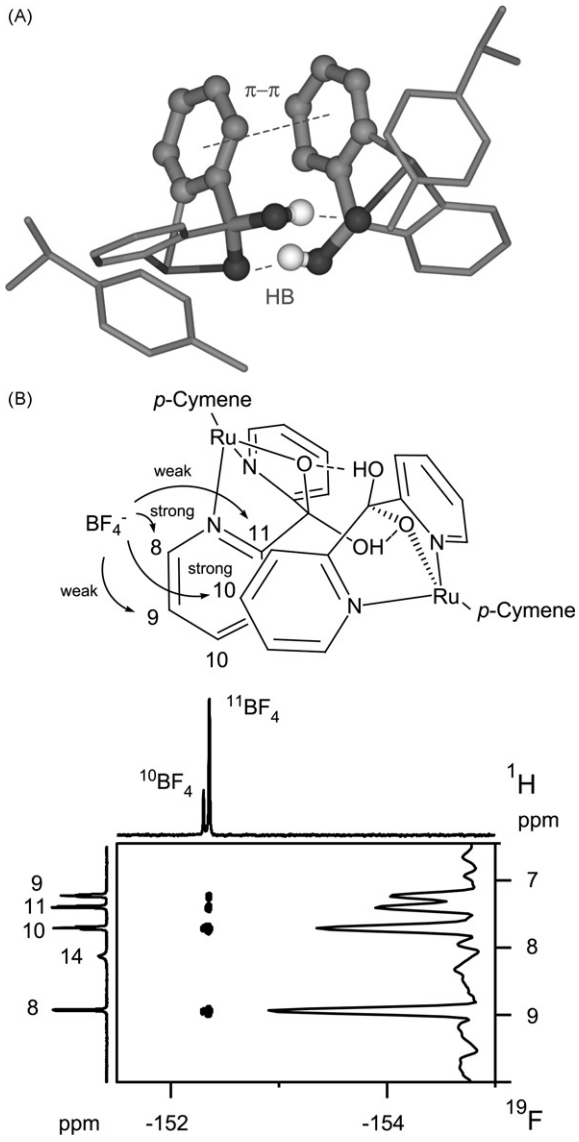


Fig. 9. (A) Intermolecular HBs and π–π stacking interaction observed in the solid state for **4Ru**$BF_4$. (B) Section of the $^{19}F,^1H$-HOESY spectrum showing the relevant interionic contacts observed in $CD_2Cl_2$ for **4Ru**$BF_4$.

the solid-state structure of **6Ru**$BPh_4$. As shown in Fig. 10A, the OH moiety of the $OCH_2CH_2OH$ tail is involved in an intracationic HB with the oxygen atom coordinated to ruthenium. If this intramolecular HB pattern is retained in solution, the OH fragment cannot establish intermolecular interactions. In agreement with the main presence of ion pairs, the anion interacts only with H8 and H9 protons of the pyridyl rings (Fig. 10B) [68,69].

### 5.1.2. Arene diamine Ru(II) complexes

Recently, the effect of HBs involving the NH moiety on the self-aggregation of some half-sandwich diamino ruthenium(II) ion pairs (Scheme 7) was investigated [13]. Sadler and coworkers proposed that NH···X HBs play a crucial role in the anticancer activity of similar half-sandwich diamino ruthenium(II) salts [70,71].

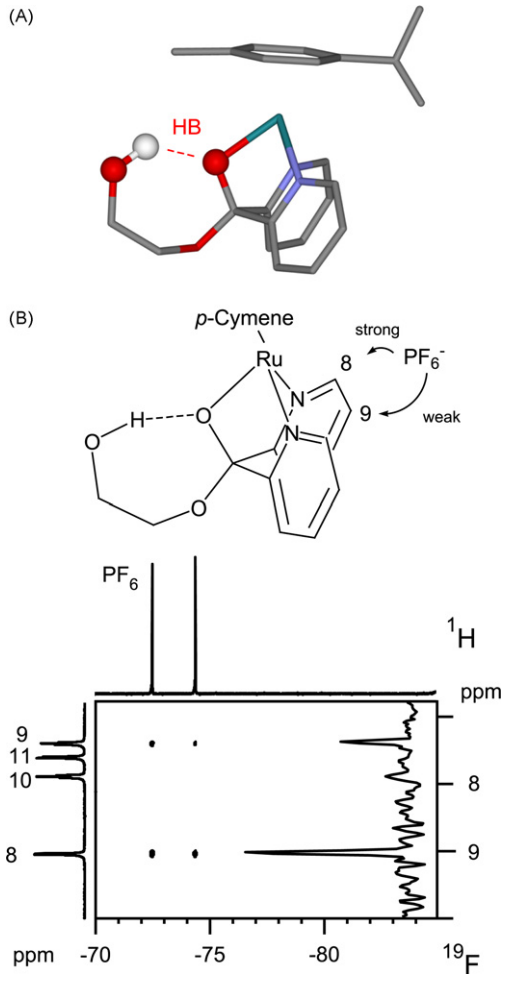


Fig. 10. (A) Intramolecular HB observed in the solid state for **6Ru**$BPh_4$. (B) Section of the $^{19}F,^{1}H$-HOESY spectrum showing the relevant interionic contacts observed in $CD_2Cl_2$ for **6Ru**$PF_6$.

Complexes **7Ru**$PF_6$ and **8Ru**$PF_6$ exhibit a remarkable tendency to self-aggregate, in a variety of solvents, that is not limited to ion pairing [13]. Complex **7Ru**$PF_6$, that contains two $NH_2$ functionalities, shows a marked tendency to form ion quadruples even in $CD_2Cl_2$ ($N^+ = N^- = 1.5$ at 4 mM). The substitution of the $NH_2$ moieties with the $NMe_2$ ones lowers the $N^+$ to 1.1 and $N^-$ to 1.0, indicating that, at a similar concentration, **8Ru**$PF_6$ is prevalently present as ion pairs. Taking into account the ion pair/ion quadruple equilibrium, the best fits of the experimental data [3] afford $K_{IQ} = 50\,M^{-1}$ ($-\Delta G^0_{IQ} = 2.2$ kcal mol$^{-1}$) and $750\,M^{-1}$ ($-\Delta G^0_{IQ} = 3.9$ kcal mol$^{-1}$) for **8Ru**$PF_6$ and **7Ru**$PF_6$,

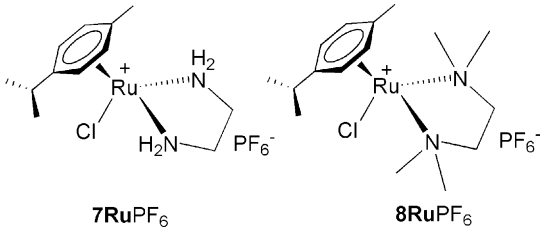


**7Ru**$PF_6$ **8Ru**$PF_6$

Scheme 7.

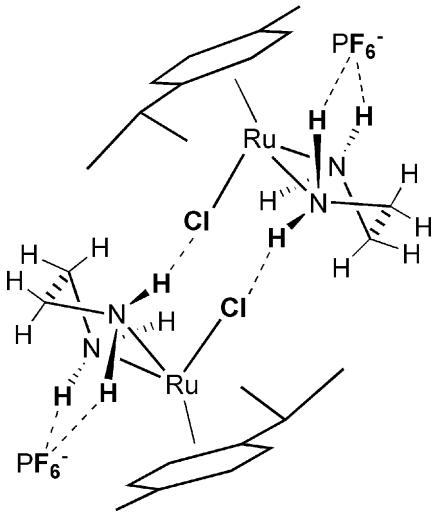


Fig. 11. A sketch of the X-ray structure of **7Ru**$PF_6$. The NH, Ru–Cl and P–F functional groups involved in HBs are drawn in bold.

respectively. This indicates that the self-aggregation is prevalently driven by HB in **7Ru**$PF_6$.

In agreement, a [1 × 1] network of intercationic hydrogen bonds between Ru–Cl and the N–H groups is found in the solid-state structure of **7Ru**$PF_6$ (Fig. 11), suggesting a preferred head-to-head [$X^-Ru^+Ru^+X^-$] arrangement of the ion quadruple. Moreover, the two N–H moieties pointing toward the cymene are committed in HBs with the $PF_6^-$ anion. Correspondingly, the $^{19}F,^{1}H$-HOESY NMR investigations indicate that the counterion is specifically located in close proximity to these $NH_2$ hydrogen atoms, giving support to the idea that the [$X^-Ru^+Ru^+X^-$] structural motif is maintained in solution.

Weaker and less specific cation–anion interactions are observed for **8Ru**$PF_6$ in $CD_2Cl_2$, indicating that **8Ru**$PF_6$ forms less intimate ion pairs than **7Ru**$PF_6$, mainly because it is impossible to establish anion–cation HBs. These observations further support a self-aggregation process driven by H-bonding in **7Ru**$PF_6$. In fact, considering the single ion pair, a larger dipole moment and a greater tendency to aggregate would have been predicted for **8Ru**$PF_6$ if the aggregation process were prevalently governed by dipole–dipole interactions.

### 5.2. Aggregation of neutral complexes

Emerging evidence suggests that H-bonding may play a significant role in the activation process of organic substrates in the second coordination sphere of a transition-metal complex [72]. For example, it has been proposed that the Noyori [73] catalysts for the transfer hydrogenation of ketones exert their action through a bifunctional mechanism involving a $Y–H^{\delta+}\cdots^{\delta-}O=C^{\delta+}\cdots^{\delta-}H–M$ (Y = NR or O, M = transition-metal) interaction, without the direct coordination of the ketone to the metal center. On the other hand, such catalysts possess all the prerequisites needed to undergo self-aggregation to form dimers and larger aggregates, because they are highly polarized and have both acceptor and donor functionalities that are suitable for establishing hydrogen bonds.

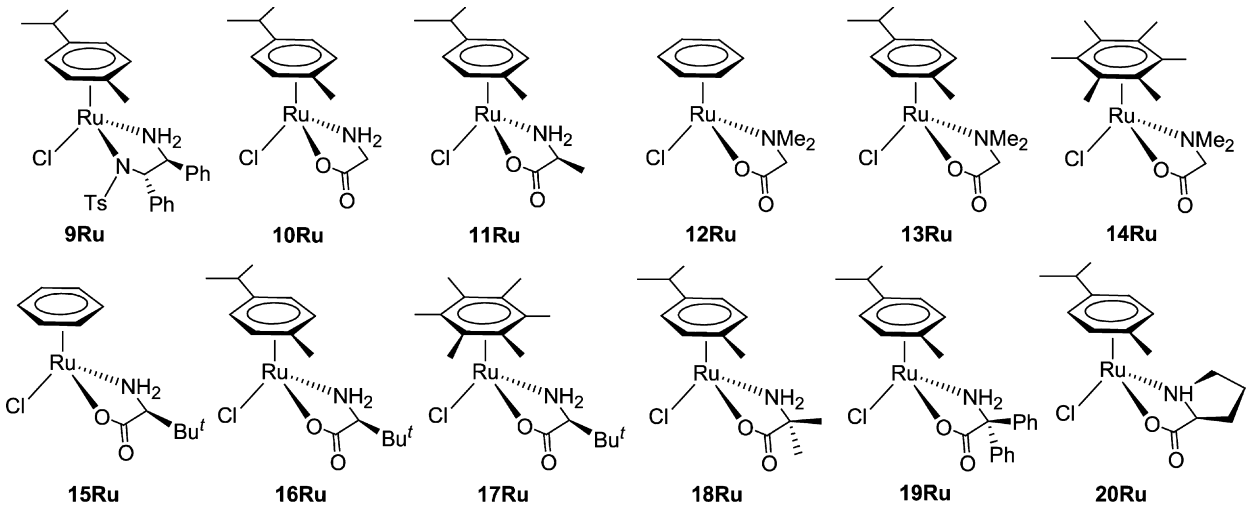


Scheme 8.

For these reasons, we recently investigated the effect of HBs on the self-aggregation properties of some catalytically relevant ruthenium(II) complexes, bearing amino-amidate [12] or amino-acidate [15,12] ligands (Scheme 8). PGSE NMR results indicate that Noyori's catalyst **9Ru**, has a marked tendency to self-aggregate in many solvents. In fact, in chloroform its $V_H$ value passes from 1073 Å$^3$ ($C = 2$ mM) to 2890 Å$^3$ ($C = 12$ mM), while in 2-propanol, that is the solvent used in catalysis, it goes from 826 Å$^3$ (0.05 mM) to 1651 Å$^3$ (42 mM). This outlines the great stability of dimers and the marked tendency to form larger aggregates as trimers and beyond. Applying the EK model to the experimental data (Fig. 12) [31,15], the equilibrium constant of the self-aggregation in 2-propanol results equal to 46 M$^{-1}$, corresponding to a $\Delta G^0 = -2.2$ kcal mol$^{-1}$. In this case, extensive NOE studies in solution did not provide any insights concerning the geometry of the aggregates.

Strong NH···OSO (2.16 Å) and $CH_{(Cym)}$···OSO (2.62 and 2.81 Å) hydrogen bonds are present between two ruthenium units in the solid-state structure of **9Ru** (Fig. 13) [74]. Starting from the X-ray crystal structure of **9Ru**, ONIOM (B3PW91:UFF) calculations were carried out on both the monomeric and dimeric structures of the complex. Given the excellent agreement between the calculated and experimental geometries, the ONIOM geometries were used in single-point calculations at the B3PW91 level to evaluate the respective monomer and dimer energies. The dimerization is exothermic by 13.4 kcal mol$^{-1}$ in the gas phase. Inclusion of the solvent as a continuum (CPCM/B3PW91) reduces the relative stability of the dimer to 2.6, 1.7 and 1.3 kcal mol$^{-1}$ in dichloromethane, methanol and acetone, respectively. Considering the dimeric structure shown in Fig. 13, other HBs may be established through the free $SO_2$ moiety or through the chlorine atoms, affording higher aggregates in solution. In agreement, infinite chains that are held together by NH···OSO and $CH_{(Cym)}$···OSO HBs are present in the solid state. To better explore the relationship between the ligand structure and HB-driven self-aggregation, we recently extended our PGSE investigations to complexes of the type [RuCl(AA)(Arene)] (AA = α-amino-acidate, **10Ru**-**20Ru**, Scheme 8) [13]. The great variety of natural and artificial aminoacids allowed the electronic and steric properties of the ligands to be easily and finely tuned. The arene and amino-acidate

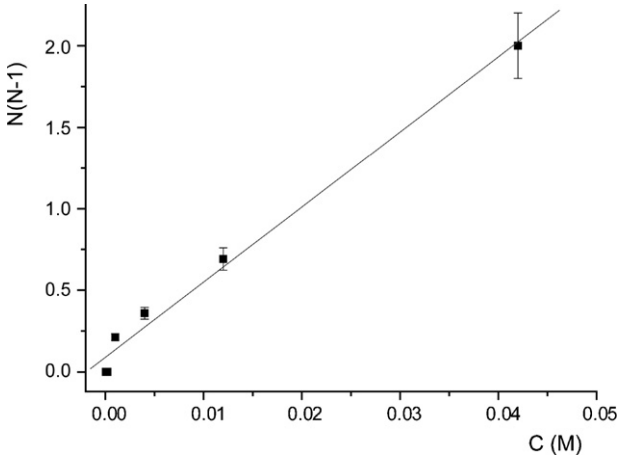


Fig. 12. Dependence of $N(N-1)$ on the concentration for **9Ru** in 2-propanol-$d_8$. The straight line fit has the following equation: $N(N-1) = 46.1C + 0.09$, $r^2 = 0.988$.

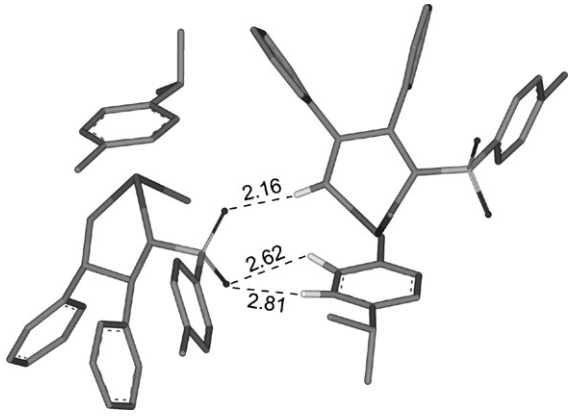


Fig. 13. Solid-state structure of **9Ru** [75] Short distances corresponding to HBs are highlighted and expressed in Å. Most hydrogen atoms have been omitted for clarity.

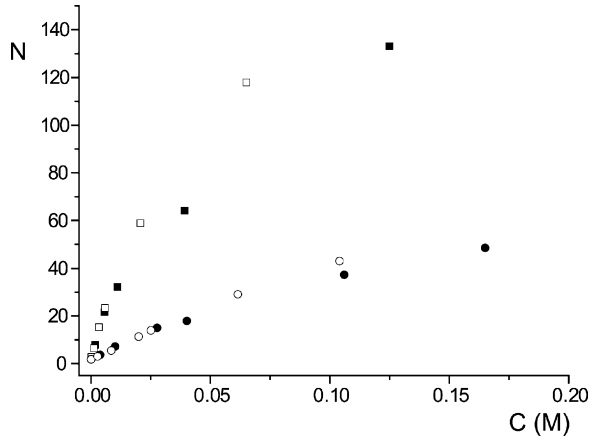


Fig. 14. Dependence of the aggregation number ($N$) on the concentration of complex **11Ru** [filled symbols: ($S_{Ru}$, $S_C$)-**11Ru**, empty ones: ($R_{Ru}$, $S_C$)-**11Ru**] in chloroform-$d$ (■, □) and dichloromethane-$d_2$ (●, ○). Using a suitable model, the $N$ values have been corrected to take into account the interstitial empty volume [15].

ligands were varied in order to selectively turn on and off the intermolecular interactions supposed to be responsible for the self-aggregation, in an attempt to identify and quantify them. Extensive investigations were carried out on complex **11Ru** that showed the highest tendency to self-aggregate, comparable only to that of **10Ru** that, however, is not very soluble in most of the organic solvents. To obtain an accurate $V_H^0$ value, complex **14Ru** was synthesized. Due to the absence of N–H HB donors and positively polarized aromatic C–Hs and to the presence of six methyl groups in the arene that hinder the π–π stacking interactions, complex **14Ru** should not self-aggregate. In fact, at low concentration, the $V_H$ of **14Ru** was equal to the van der Waals volume in both chloroform and methylene chloride, so, in this case, $V_H^0$ was set equal to $V_{vdW}$ for all other complexes. **10Ru** and **11Ru**, having all "sources" of aggregation on, showed an extraordinary tendency to self-aggregate. In $CDCl_3$, at the highest investigated concentration (125 mM), **11Ru** showed an average aggregate with $r_H = 2.08$ nm and $N = 133$ (Fig. 14), while at the lowest concentration (0.2 mM) it was mainly present as dimers and trimers ($r_H = 0.54$ nm, $N = 2.7$). As the polarity of the solvent increased smaller, but still remarkable, aggregates were observed. In fact, the level of aggregation decreased by about a third on passing from chloroform to methylene chloride (Fig. 14) and by a tenth from chloroform to acetone, while the protic 2-propanol further reduced $N$. The HB between the aminic protons and the chlorine or the carboxylate moieties is the most important interaction, in fact the highest levels of aggregation are shown for complexes **10Ru**, **11Ru**, **15Ru**, **16Ru** and **17Ru**, that have the $NH_2$ moiety.

Nevertheless, the steric requirements of both the ligand and the arene play an important role in modulating the level of self-aggregation. The value of $N$ decreases as the steric hindrance of the ligand increases in the series **10Ru**, **11Ru**, **16Ru**, **18Ru** and **19Ru**. A similar decrease in the $N$ value is observed as the hindrance of the arene increases (**15Ru**, **16Ru**, **17Ru**).

Only one aminic proton is present in **20Ru**, but its orientation is decisive in determining $N$: in this case, the two epimers

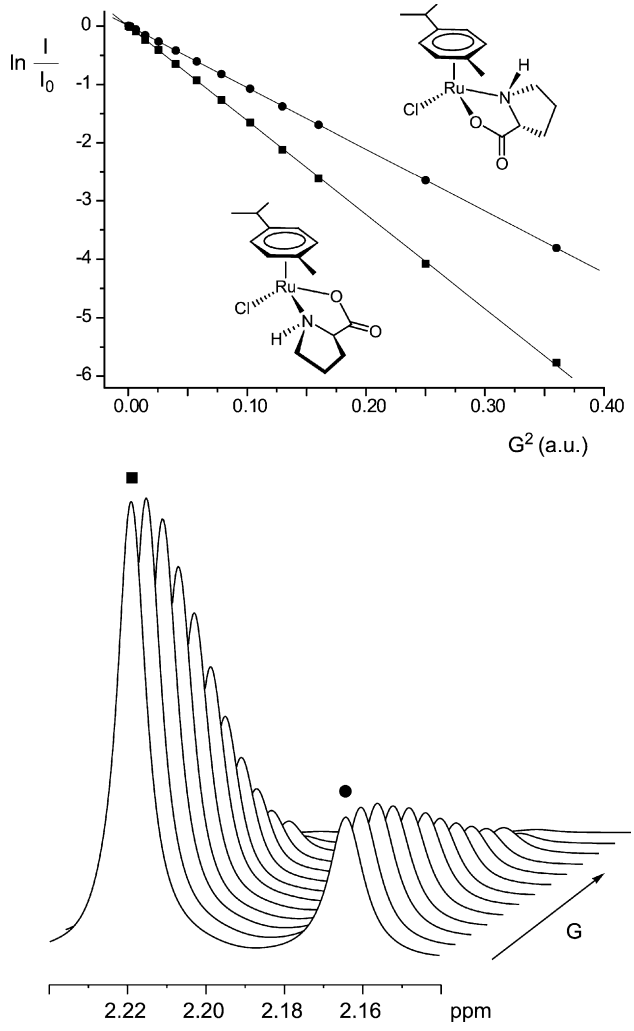


Fig. 15. A section of $^1$H-PGSE NMR spectra recorded in $CDCl_3$ showing the dependence of the resonance intensities (methyl protons of cymene for ($S_{Ru}$, $S_N$, $S_C$)-**20Ru** (■) and ($R_{Ru}$, $S_N$, $S_C$)-**20Ru**) (●) on the strength of the pulsed field gradient ($G$) and the relative plot of ln($I$/$I_0$) *versus* $G^2$ (on the top).

($S_{Ru}$, $S_N$, $S_C$)-**20Ru** and ($R_{Ru}$, $S_N$, $S_C$)-**20Ru** show very different behaviors. This is illustrated in Fig. 15 where the intensity of one $^1$H resonance relative to ($S_{Ru}$, $S_N$, $S_C$)-**20Ru** shows a much more marked decrease, as the pulsed field gradient increases, than the analogous resonance relative to ($R_{Ru}$, $S_N$, $S_C$)-**20Ru**. In $CDCl_3$, the former had a maximum $N$ value equal to 10.6 (178 mM), while for the latter $N = 29.0$ (71 mM). In the ($S_{Ru}$, $S_N$, $S_C$) isomer the aminic proton is probably engaged in an intramolecular HB with the chlorine atom and is not completely available to undergo intermolecular interactions. A diastereoisomeric intermolecular recognition process appears to be present in solution.

A limited tendency to self-aggregate is also observed for both **12Ru** and **13Ru** bearing the $NMe_2$ group; in the absence of the $NH_2$ HB donor, association can be driven by the aromatic C–H···Cl electrostatic interaction described by Brunner [75], or by π–π stacking between two arene moieties.

All the interactions responsible for the aggregation can be easily identified in the solid state: for example, in the crystal

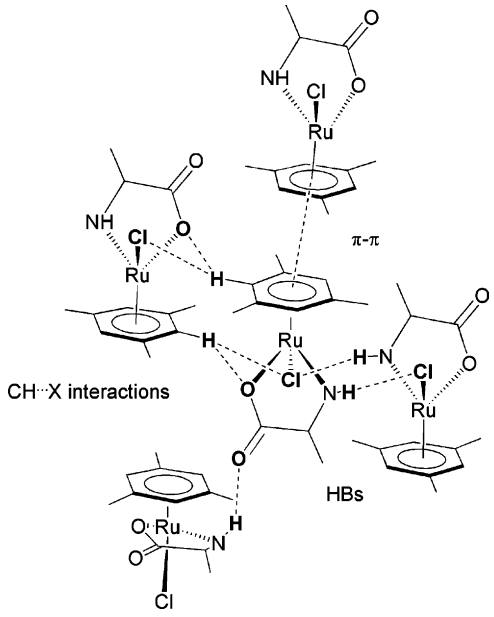


Fig. 16. A sketch of the X-ray structure of RuCl(Mes)(S-Ala), published by Carter et al. Atoms involved in non-covalent interactions are draw in bold [76].

Table 1
Equilibrium constants ($K$) and free energies of the aggregation process ($\Delta G^0$) for some compounds in different solvents

| Compound | Solvent | $K$ ($M^{-1}$) | $-\Delta G^0$ (kcal mol$^{-1}$) |
|---|---|---|---|
| **11Ru** | $CDCl_3$ | 170,000 | 7.1 |
| **11Ru** | $CD_2Cl_2$ | 14,500 | 5.6 |
| **11Ru** | Acetone-$d_6$ | 780 | 3.9 |
| **11Ru** | 2-Propanol-$d_8$ | 170 | 3.0 |
| **13Ru** | $CDCl_3$ | 25 | 1.9 |
| **16Ru** | $CDCl_3$ | 15,600 | 5.7 |
| **18Ru** | $CD_2Cl_2$ | 450 | 3.6 |
| ($S_{Ru}$, $S_N$, $S_C$)-**20Ru** | $CDCl_3$ | 320 | 3.4 |
| ($R_{Ru}$, $S_N$, $S_C$)-**20Ru** | $CDCl_3$ | 7,600 | 5.2 |

packing of RuCl(*S*-Ala)(Mes) [76] each molecule is surrounded by four other molecules and undergoes HBs (NH···Cl and NH···O), CH-X interactions (CH···Cl and CH···O) and π–π stacking (Fig. 16).

An estimation of the association equilibrium constants ($K$) and $\Delta G^0$ was obtained for some complexes through the EK model (Table 1).

The difference in $\Delta G^0$ for **11Ru** and **13Ru** ($|\Delta(\Delta G^0)|$) is equal to 5.3 kcal mol$^{-1}$ and is consistent with the energy of two "classical" HBs in chloroform. $\Delta G^0$ for the aggregation of ($S_{Ru}$, $S_N$, $S_C$)-**20Ru** and ($R_{Ru}$, $S_N$, $S_C$)-**20Ru** diastereoisomers (−3.4 and −5.2 kcal mol$^{-1}$, respectively) are rather different and reflect their markedly different tendency to self-aggregate. If these values are compared with $\Delta G^0$ for the aggregation of **11Ru** (7.1 kcal mol$^{-1}$), it can be seen that the substitution of the proton pointing toward cymene leads to $|\Delta(\Delta G^0)| = 3.7$ kcal mol$^{-1}$, while the substitution of the proton pointing toward the chlorine gives $|\Delta(\Delta G^0)| = 1.9$ kcal mol$^{-1}$. The $|\Delta(\Delta G^0)|$ between **11Ru** and **16Ru** (1.4 kcal mol$^{-1}$) accounts for the destructive contribution of steric hindrance.

## 6. Conclusions

Herein we have shown that all types of non-covalent interactions, under "certain" circumstances, may cause the self-aggregation of coordination compounds in solution. Even when coordination compounds cannot establish HB and π–π stacking interactions and do not have any intrinsic permanent dipole moment associated with the ion pair, they can self-aggregate provided that a network of dispersive forces can act cooperatively. This usually occurs for large molecules. The "switching on" of the permanent dipolar moment, as in transition-metal complex ion pairs, furnishes an additional force that makes it the formation of quadrupoles and higher aggregates possible in solvent with low relative permittivity. If the proper functionalities for HB and π–π stacking are introduced, self-aggregation may occur in solvents with higher relative permittivity and nanometric aggregates can form.

The results discussed here mainly come from the application of PGSE NMR spectroscopy that demonstrated to be a very powerful tool. It not only allows the average hydrodynamic dimension to be determined, but the thermodynamic parameters of the self-aggregation processes can also be derived, once the hydrodynamic dimension of the single aggregating unit has been correctly evaluated [3].

## Acknowledgments

We are indebted to all graduate and PhD students who have contributed to obtaining the results herein reported. Special thanks are due to Eric Clot (CNRS Montpellier, France) who performed all the calculations discussed in the review. Many thanks are also due to Elisabetta Foresti and Piera Sabatino (University of Bologna, Italy) for having determined some solid-state structures. We thank the Ministero dell'Università e della Ricerca (MUR, Rome, Italy) and the Dow Chemical Company for support.

## References

[1] D. Neuhaus, M. Williamson, The Nuclear Overhauser Effect in Structural and Conformational Analysis, Wiley–VCH, 2000.
[2] P. Stilbs, Prog. Nucl. Magn. Reson. Spectrosc. 19 (1987) 1;
W.S. Price, Concepts Magn. Res. 9 (1997) 299;
W.S. Price, Concepts Magn. Reson. 10 (1998) 197;
C.S. Johnson Jr., Prog. Nucl. Magn. Reson. Spectrosc. 34 (1999) 203.
[3] A. Macchioni, G. Ciancaleoni, C. Zuccaccia, D. Zuccaccia, Chem. Soc. Rev., 2008, doi:10.1039/B615067P.
[4] G. Bellachioma, G. Cardaci, A. Macchioni, G. Reichenbach, S. Terenzi, Organometallics 15 (1996) 4349;
A. Macchioni, G. Bellachioma, G. Cardaci, V. Gramlich, H. Rüegger, S. Terenzi, L.M. Venanzi, Organometallics 16 (1997) 2139.
[5] A. Macchioni, Chem. Rev. 105 (2005) 2039;
S.D. Bergman, R. Frantz, D. Gut, M. Kol, J. Lacour, Chem. Commun. (2006) 850;
G.L. Hamilton, E.J. Kang, M. Mba, F.D. Toste, Science 317 (2007) 496;
M.G. Basallote, M. Besora, C.E. Castillo, M.J. Fernandez-Trujillo, A. Lledos, F. Maseras, M.A. Manez, J. Am. Chem. Soc. 129 (2007) 6608;
B. Binotti, G. Bellachioma, G. Cardaci, C. Carfagna, C. Zuccaccia, A. Macchioni, Chem. Eur. J. 13 (2007) 1570.
[6] A. Macchioni, Eur. J. Inorg. Chem. (2003) 195, and references therein.

[7] T. Beringhelli, G. D'Alfonso, D. Maggioni, P. Mercandelli, A. Sironi, Chem. Eur. J. 11 (2005) 650.
[8] C. Zuccaccia, G. Bellachioma, G. Cardaci, A. Macchioni, Organometallics 19 (2000) 4663.
[9] M. Valentini, P.S. Pregosin, H. Ruegger, Dalton 24 (2000) 4507.
[10] S. Beck, A. Geyer, H.H. Brintzinger, Chem. Commun. (1999) 2477.
[11] D. Zuccaccia, S. Sabatini, G. Bellachioma, G. Cardaci, E. Clot, A. Macchioni, Inorg. Chem. 42 (2003) 5465.
[12] D. Zuccaccia, E. Clot, A. Macchioni, New J. Chem. 29 (2005) 430.
[13] D. Zuccaccia, A. Macchioni, Organometallics 24 (2005) 3476.
[14] A. Macchioni, A. Romani, C. Zuccaccia, G. Guglielmetti, C. Querci, Organometallics 22 (2003) 1526.
[15] G. Ciancaleoni, I. Di Maio, D. Zuccaccia, A. Macchioni, Organometallics 26 (2007) 489.
[16] B. Binotti, A. Macchioni, C. Zuccaccia, D. Zuccaccia, Comments Inorg. Chem. 23 (2002) 417.
[17] P.S. Pregosin, P.G.A. Kumar, I. Fernández, Chem. Rev. 105 (2005) 2977.
[18] P.S. Pregosin, Prog. Nucl. Magn. Reson. Spectrosc. 49 (2006) 261.
[19] G. Ciancaleoni, C. Zuccaccia, D. Zuccaccia, A. Macchioni, Organometallics 26 (2007) 3624.
[20] C.A. Kraus, J. Phys. Chem. 60 (1956) 129.
[21] D.T. Copenhafer, C.A. Kraus, J. Am. Chem. Soc. 73 (1951) 4557.
[22] D. Zuccaccia, G. Bellachioma, G. Cardaci, G. Ciancaleoni, C. Zuccaccia, E. Clot, A. Macchioni, Organometallics 26 (2007) 3930.
[23] $N^+$ and $N^-$ are the ratios between the measured hydrodynamic volumes of the cationic and anionic moieties, respectively, over the hydrodynamic volume of the ion pair.
[24] E. Clot, A. Macchioni et al., unpublished results.
[25] F. Maseras, K. Morokuma, J. Comput. Chem. 16 (1995) 1170;
S. Humbel, S. Sieber, K. Morokuma, J. Chem. Phys. 16 (1996) (1959);
M. Svensson, S. Humbel, R.D.J. Froese, T. Matsubara, S. Sieber, K. Morokuma, J. Phys. Chem. 100 (1996) 19357;
T. Vreven, K. Morokuma, J. Comput. Chem. 21 (2000) 1419.
[26] J.A. Gladysz (Ed.), Chem. Rev. 100 (2000) 1167, special issue on Frontiers in Metal-Catalyzed Polymerization.;
T.J. Marks and J.C. Stevens (Eds.), Topics Catal. 7 (1999) 1, special issue on Metallocene and Related Catalysts.
[27] C. Zuccaccia, N.G. Stahl, A. Macchioni, M.-C. Chen, J.A. Roberts, T.J. Marks, J. Am. Chem. Soc. 126 (2004) 1448.
[28] Original $D_t$ data were re-elaborated using a more accurate value for $D_{TPTS}$ in benzene ($7.54 \times 10^{-10}$ m$^2$ s$^{-1}$); the corresponding hydrodynamic volume ($V_H$) calculated at the lowest concentration was assumed to be that of the single ion pair ($V_H^0$).
[29] (a) E.Y.X. Chen, T.J. Marks, Chem. Rev. 100 (2000) 1391;
(b) P.A. Wilson, M.H. Hannant, J.A. Wright, R.D. Cannon, M. Bochmann, Macromol. Symp. 236 (2006) 100.
[30] (a) G. Lanza, I.L. Fragala', T.J. Marks, Organometallics 21 (2002) 5594;
(b) K. Vranka, T. Ziegler, Organometallics 20 (2001) 905.
[31] R.B. Martin, Chem. Rev. 96 (1996) 3043.
[32] A. Correa, L. Cavallo, J. Am. Chem. Soc. 128 (2006) 10952.
[33] D.E. Babushkin, H.H. Brintzinger, J. Am. Chem. Soc. 124 (2002) 12869.
[34] The experimentally determined $r_H$ for $[Cp_2Zr(\mu\text{-}Me)_2AlMe_2]^+MeMAO^-$ at $4.8 \times 10^{-5}$ M (12.2 Å) was used to calculate $V_H^0$ (7606 Å$^3$) of the single ion pair assuming a spherical shape.
[35] I.I. Zakharov, V.A. Zakharov, Macromol. Theory Simul. 11 (2002) 352, and references therein.
[36] F. Song, S.J. Lancaster, R.D. Cannon, M. Schormann, S.M. Humphrey, C. Zuccaccia, A. Macchioni, M. Bochmann, Organometallics 24 (2005) 1315.
[37] C. Alonso-Moreno, S.J. Lancaster, C. Zuccaccia, A. Macchioni, M. Bochmann, J. Am. Chem. Soc. 129 (2007) 9282.
[38] *N* values for **11Zr**BT were recalculated by contrasting the reported hydrodynamic volumes ($V_H = 1304$ Å$^3$, see Ref. [36]) with a more reliable hydrodynamic volume for the single ion pair ($V_H^0 = 966$ Å$^3$, Ref. [37]).
[39] S. Beck, S. Lieber, F. Schaper, A. Geyer, H.H. Brintzinger, J. Am. Chem. Soc. 123 (2001) 1483.
[40] F. Song, R.D. Cannon, S.J. Lancaster, M. Bochmann, J. Mol. Catal. 218 (2004) 21.
[41] F. Song, R.D. Cannon, M. Bochmann, J. Am. Chem. Soc. 125 (2003) 7641.
[42] I. Krossing, I. Raabe, Angew. Chem., Int. Ed. Engl. 43 (2004) 2066.
[43] D. Zuccaccia, L. Busetto, M.C. Cassani, A. Macchioni, R. Mazzoni, Organometallics 25 (2006) 2201.
[44] L. Busetto, M.C. Cassani, P.W.N.M. Van Leeuwen, R. Mazzoni, Dalton Trans. (2004) 2767.
[45] (a) C.A. Hunter, J.K.M. Sanders, J. Am. Chem. Soc. 112 (1990) 5525;
(b) A.S. Shetty, J. Zhang, J.S. Moore, J. Am. Chem. Soc. 118 (1996) 1019, and references therein.
[46] J.-M. Lehn, Supramolecular Chemistry: Concepts and Perspectives, VCH, New York, 1995;
L.F. Lindoy, I.M. Atkinson, Self-Assembly in Supramolecular Systems, Cambridge University Press, UK, 2000;
I. Haiduc, F.T. Edelman, Supramolecular Organometallic Chemistry, Wiley–VCH, 1999;
D.J. Hill, M.J. Mio, R.B. Prince, T.S. Hughes, J.S. Moore, Chem. Rev. 101 (2001) 3893;
M.A. Omary, A.A. Mohamed, M.A. Rawashdeh-Omary, J.P. Fackler Jr., Coord. Chem. Rev. 249 (2005) 1372.
[47] S. Bhattacharya, K. Tominaga, T. Kimura, H. Uno, N. Komatsu, Chem. Phys. Lett. 433 (2007) 395;
A. Petitjean, R.G. Khoury, N. Kyritsakas, J.M. Lehn, J. Am. Chem. Soc. 126 (2004) 6637;
A. Sygula, F.R. Fronczek, R. Sygula, P.W. Rabideau, M.M. Olmstead, J. Am. Chem. Soc. 129 (2007) 3842.
[48] W.I. White, Aggregation of porphyrins and metalloporphyrins. In: D. Dolphin (Ed.), The Porphyrins, vol. 5. New York Academic Press, 1978;
K. Kano, K. Fukuda, H. Wakami, R. Nishiyabu, R.F. Pasternack, J. Am. Chem. Soc. 122 (2000) 7494;
K. Kano, H. Minamizono, T. Kitae, S. Negi, J. Phys. Chem. A 101 (1997) 6118.
[49] W. Saenger, Principles of Nucleic Acid Structure, Springer-Verlag, New York, 1984, p. 132.
[50] R.F. Pasternack, E.J. Gibbs. Porphyrin and metalloporphyrin interactions with nucleic acids. In: A. Sigel, H. Sigel (Eds.), Metal Ions in Biological Systems, vol. 33. Marcel Dekker, New York, 1996, p. 367.
[51] F. Scandola, M.T. Indelli, C. Chiorboli, C.A. Bignozzi, Top. Curr. Chem. 158 (1990) 73;
(b) V. Balzani, A. Juris, M. Venturi, S. Campagna, S. Serroni, Chem. Rev. 96 (1996) 759.
[52] F. Jaekle, Dalton Trans. 27 (2007) 2851.
[53] K.E. Erkkila, D.T. Odom, J.K. Barton, Chem. Rev. 99 (1999) 2777.
[54] D. Gut, A. Rudi, J. Kopilov, I. Goldberg, M. Kol, J. Am. Chem. Soc. 124 (2002) 5449;
S.D. Bergman, I. Goldberg, A. Barbieri, F. Barigelletti, M. Kol, Inorg. Chem. 43 (2004) 2355;
S.D. Bergman, D. Reshef, L. Frish, Y. Cohen, I. Goldberg, M. Kol, Inorg. Chem. 43 (2004) 3792.
[55] J. Moussa, K.M.-C. Wong, L.-M. Chamoreau, H. Amouri, V.W.-W. Yam, Dalton Trans. (2007) 3526;
V.W.-W. Yam, K.M.-C. Wong, N. Zhu, J. Am. Chem. Soc. 124 (2002) 6506.
[56] G. Arena, L. Monsù Scolaro, R.F. Pasternack, R. Romeo, Inorg. Chem. 34 (1995) 2994.
[57] G. Arena, G. Calogero, S. Campagna, L. Monsù Scolaro, V. Ricevuto, R. Romeo, Inorg. Chem. 37 (1998) 2763;
M. Casamento, G.E. Arena, C. Lo Passo, I. Pernice, A. Romeo, L. Monsù Scolaro, Inorg. Chim. Acta 275-276 (1998) 242.
[58] R. Romeo, L. Monsù Scolaro, M.R. Plutino, A. Albinati, J. Organomet. Chem. 593–594 (2000) 403.
[59] T. Steiner, Angew. Chem., Int. Ed. 41 (2002) 48, and reference therein.
[60] G.A. Jeffrey, An introduction to Hydrogen Bonding, Oxford University Press, Oxford, 1997.
[61] D. Braga, F. Grepioni, G.R. Desiraju, Chem. Rev. 98 (1998) 1375.
[62] P.D. Beer, Acc. Chem. Res. 31 (1998) 71;
P.D. Beer, P.A. Gale, Angew. Chem., Int. Ed. 40 (2001) 486.
[63] J.L. Boyer, M.L. Kuhlman, T.B. Rauchfuss, Acc. Chem. Res. 40 (2007) 233.

[64] M. Cametti, M. Nissinen, A. Dalla Cort, L. Mandolini, K. Rissanen, J. Am. Chem. Soc. 129 (2007) 3641;
P.A. Gale, Coord. Chem. Rev. 240 (2003) 191.
[65] R. Noyori, M. Yamakawa, S. Hashiguchi, J. Org. Chem. 66 (2001) 7931;
P. Pelagatti, M. Carcelli, F. Calbiani, C. Cassi, L. Elviri, C. Pelizzi, U. Rizzotti, D. Rogolino, Organometallics 24 (2005) 5836.
[66] R.H. Fish, G. Jaouen, Organometallics 22 (2003) 2166;
K. Severin, R. Bergs, W. Beck, Ang. Chem., Int. Ed. 37 (1998) 1635;
G. Jaouen, W. Beck, Bioorganometallics (2006) 1;
R. Alberto, Top. Curr. Chem. 252 (2005);
M. Melchart, P.J. Sadler, Bioorganometallics (2006) 39;
T. Ward, Chem. Eur. J. 11 (2005) 3798.
[67] D. Zuccaccia, E. Foresti, S. Pettirossi, P. Sabatino, C. Zuccaccia, A. Macchioni, Organometallics 26 (2007) 6099.
[68] D. Zuccaccia, G. Bellachioma, G. Cardaci, C. Zuccaccia, A. Macchioni, Dalton Trans. (2006) 1963.
[69] G. Ciancaleoni, G. Bellachioma, G. Cardaci, G. Ricci, R. Ruzziconi, D. Zuccaccia, A. Macchioni, J. Organomet. Chem. 691 (2006) 165.
[70] R.E. Morris, R.E. Aird, M. Piedad del Socorro, H. Chen, J. Cumming, N. Hughes, S. Parson, A. Parkin, G. Boyd, D.L. Jodrell, P.J. Sadler, J. Med. Chem. 44 (2001) 1652.
[71] O. Novakova, H. Chen, O. Vrana, A. Rodger, P.J. Sadler, V. Brabek, Biochemistry 42 (2003) 11544;
H. Chen, R.E. Morris, P.J. Sadler, J. Am. Chem. Soc. 125 (2003) 173.
[72] M. Sawamura, Y. Ito, Chem. Rev. 92 (1992) 857.
[73] R. Noyori, S. Hashiguchi, Acc. Chem. Res. 30 (1997) 97.
[74] K.-J. Haack, S. Hashiguchi, A. Fujii, T. Ikariya, R. Noyori, Angew. Chem., Int. Ed. 36 (1997) 285.
[75] H. Brunner, M. Weber, M. Zabel, T. Zwack, Angew. Chem., Int. Ed. 42 (2003) 1859;
H. Brunner, M. Weber, M. Zabel, Coord. Chem. Rev. 242 (2003) 3.
[76] L.C. Carter, D.L. Davies, K.T. Duffy, J. Fawcett, D.R. Fawcett, Acta Crystallogr. C C50 (1994) 1559.